Neutron clustering: spatial fluctuations in multiplying systems at the critical point

A. Zoia, E. Dumonteil

M&C 2017 - International Conference on Mathematics & Computational Methods Applied to Nuclear Science & Engineering, Jeju, Korea, April 16-20, 2017, on USB (2017)

Neutron clustering: spatial fluctuations in multiplying systems at the critical point

Andrea Zoia,[*], Eric Dumonteil,[†]

[*]*Den-Service d'études des réacteurs et de mathématiques appliquées (SERMA), CEA, Université Paris-Saclay, F-91191, Gif-sur-Yvette, France*

[†]*IRSN, 31 Avenue de la Division Leclerc, 92260 Fontenay aux Roses, France*

Corresponding author: andrea.zoia@cea.fr

Abstract - *We investigate the spatial fluctuations of a neutron population close to criticality: the interplay between random births and deaths leads to a spontaneous clustering of the diffusing individuals. By resorting to a statistical mechanics approach, we determine the behaviour of the average neutron neutron density, the pair correlation function and other relevant physical observables. When the individuals are left free to evolve, their ultimate fate is the so-called critical catastrophe, i.e., extinction. When a global constraint is imposed on the total number of individuals, the impact of clustering on diffusion depends on the competition between the time required for a neutron to explore the whole reactor, and the time over which the population has undergone a full generational renewal. In order to illustrate these results, exact formulas and scaling functions are derived for a simple model of nuclear reactor and are compared to Monte Carlo simulations.*

I. INTRODUCTION

Self-sustaining chains of neutrons in nuclear reactors form a prototypical example of a system operating at the critical point [1, 2]. At criticality, which means when births by fission are exactly compensated by losses by capture and leakage, the interplay between the fluctuations stemming from birth-death events and those stemming from random displacements subtly affects the *spatial distribution* of the particles in such systems. This is particularly important during start-up using weak sources: although the population may eventually rise to a level where fluctuations are negligible, yet their effect might persist for long times due to the impact on the initial conditions [2]. The analysis of this statistical behaviour is typically carried out by developing the evolution equations for the first few moments of the neutron population [1, 2, 3, 4].

The physical mechanisms underlying the complex nature of the moment equations can be probed by Monte Carlo simulation. In particular, it has been recently shown that at and close to the critical point a collection of neutrons, although spatially uniform at the initial time, may eventually display a highly non-Poisson patchiness (see Fig. 1) [5].

The emergence of such *neutron clustering* due to the competition between fission, capture and diffusion has been first investigated in [6], based on a formal analogy with the behaviour of ecological communities [7, 8, 9, 10, 11], and later extended to take into account finite-size effects [12], population control [13] and the impact of delayed neutrons [14]. In this work we will revisit the basic findings about neutron clustering and single out the key ingredients that govern the spatial fluctuations.

II. A SIMPLE MODEL OF A MULTIPLYING SYSTEM

In order to illustrate the features of neutron clustering, we will introduce a simplified model of a multiplying system that yet retains all the key ingredients. Neutrons will be represented as a collection of particles undergoing random diffusion, reproduction and capture within a homogeneous

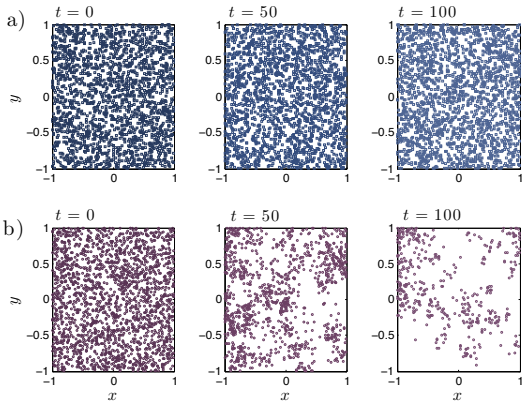

Fig. 1. Monte Carlo simulation of neutrons in a two-dimensional box with reflecting boundaries. At $t = 0$, the spatial particle distribution is uniform. In case *a*), particles obey regular Brownian motion: the spatial distribution stays uniform. In case *b*), particles obey a binary branching Brownian motion with equal birth and death rates: particles spontaneously form random clusters. Eventually, the entire population goes to extinction.

d-dimensional box of finite volume $V = L^d$, L being the linear size. To simplify the matter, the box will have perfectly reflecting boundaries. The stochastic paths of neutrons are known to follow position and velocity dependent exponential flights [2]. For our model, we approximate these paths by d-dimensional branching Brownian motions with a constant diffusion coefficient D. The diffusing walker undergoes capture at rate γ and reproduction at rate β. In this latter case, the neutron disappears and is replaced by a random number k of descendants, distributed according to a law p_k with average $\nu_1 = \sum_k k p_k$. We are assuming here that all fission neutrons are prompt, so as to keep notation to a minimum: the effects of precursors will be included later.

At the critical point, we must have $\gamma = \beta(\nu_1 - 1)$, i.e., losses compensate births. In this regime, the Galton-Watson

theory shows that the total number $N(t)$ of particles in the system stays constant on average, i.e., $\mathbb{E}[N(t)] = N_0$, whereas the variance grows in time, i.e., $\sigma_t^2[N] = \mathbb{E}[N^2(t)] - \mathbb{E}^2[N(t)] \propto \beta N_0 t$. This implies that the typical fluctuations of the whole population size, say $\sigma_t[N]$, will become comparable to the average value N_0 over a time $t \sim N_0/\beta$: then, a single fluctuation is capable of killing the entire population [1]. In the context of reactor physics, the extinction of the fission chains at criticality goes under the name of *critical catastrophe* [2]. In the following, we will show how the spatial distribution of neutrons within the box is affected by the fission-chain fluctuations.

III. THE PHYSICAL OBSERVABLES

Let us denote by $n(\mathbf{x}, t)$ the instantaneous density of neutrons located at $\mathbf{x}$ at time t. The evolution equations for the statistical moments of $n(\mathbf{x}, t)$ can be derived by resorting to the Pál-Bell equations [1], which can be regarded as a particular case of the more general Feynman-Kac path-integral approach [12]. Both strategies are based on the the reciprocity property of random walks [4, 1, 2]: the idea is to write down the equations governing the probability generating functions for $n(\mathbf{x}, t)$, from which the average particle density and the correlations can be obtained by simple derivation (some hints are provided in the Appendix).

Let us denote by $\mathcal{G}_t(\mathbf{x}; \mathbf{x}_0)$ the Green's function satisfying the backward equation

$$\frac{\partial}{\partial t}\mathcal{G}_t(\mathbf{x}; \mathbf{x}_0) = \mathcal{L}^\dagger_{\mathbf{x}_0}\mathcal{G}_t(\mathbf{x}; \mathbf{x}_0), \tag{1}$$

where

$$\mathcal{L}^\dagger_{\mathbf{x}_0} = D\nabla^2_{\mathbf{x}_0} + \beta(\nu_1 - 1) - \gamma, \tag{2}$$

with the boundary conditions of the problem at hand and the initial condition $\mathcal{G}_0(\mathbf{x}; \mathbf{x}_0) = \delta(\mathbf{x} - \mathbf{x}_0)$. Intuitively, the Green function physically represents the average number of particles appearing at $\mathbf{x}$ at time t for a single particle started at $\mathbf{x}_0$ at $t = 0$, or equivalently the average number of particles originally present at $\mathbf{x}_0$ at $t = 0$ for a single particle detected at $\mathbf{x}$ at time t, by the reciprocity theorem [4]. The average neutron density $\psi_t(\mathbf{x})$ at a point $\mathbf{x}$ can be expressed as

$$\psi_t(\mathbf{x}) = \mathbb{E}[n(\mathbf{x}, t)] = N \int d\mathbf{x}_0 q(\mathbf{x}_0)\mathcal{G}_t(\mathbf{x}; \mathbf{x}_0), \tag{3}$$

where N is the number of individuals composing the initial neutron population, and q is the spatial probability distribution function of each neutron at time $t = 0$ (assuming independence) [12]. For a *critical* reactor, $\beta(\nu_1 - 1) = \gamma$ and we thus have $\mathcal{L}^\dagger_{\mathbf{x}_0} = D\nabla^2_{\mathbf{x}_0}$. In order to simplify the forthcoming discussion, it is convenient to require that the initial spatial distribution in the box is uniform, namely, $q = 1/V$. This corresponds to taking the population at equilibrium compatibly with the assigned mass-preserving boundary conditions at $t = 0$. Then, from Eq. (3) we would therefore have a flat average density $\psi_t(\mathbf{x}) = N/V = \psi_0$ at any time, insensitive to local fluctuations.

[1] Strictly speaking, the mean extinction time of a critical system is infinite. Here we are providing a heuristic argument based on a typical time [7].

The analysis of the spatial inhomogeneities shown in Fig. 1 can be carried out by resorting to the two-point correlation function $h_t(\mathbf{x}, \mathbf{y}) = \mathbb{E}[n(\mathbf{x}, t)n(\mathbf{y}, t)]$, which is proportional to the joint probability density for particle pairs simultaneously occupying positions $\mathbf{x}$ and $\mathbf{y}$ [1, 2]. The correlation length can be extracted from the shape of the function h: if h is almost flat in space, then the correlations will have the same relevance at any spatial site; on the contrary, spatial clustering will be mirrored in a peak at $\mathbf{x} \simeq \mathbf{y}$, i.e., an increased probability of finding particles lying at short distances [12, 13]. The overall intensity of the correlations is simply provided by the amplitude of h.

The function $h_t(\mathbf{x}, \mathbf{y})$ can be generally written as $h_t = h_t^{id} + \tilde{h}_t$, where h_t^{id} is the contribution from independent trajectories, and $\tilde{h}_t$ is the contribution of the trajectories correlated via a fission event. For the former, we have

$$h_t^{id}(\mathbf{x}, \mathbf{y}) = c_N\psi_t(\mathbf{x})\psi_t(\mathbf{y}) + \psi_t(\mathbf{x})\delta(\mathbf{x} - \mathbf{y}), \tag{4}$$

including self-correlations, where $c_N = (N - 1)/N \simeq 1$ for large $N \gg 1$ [12]. For the latter, we have

$$\tilde{h}_t(\mathbf{x}, \mathbf{y}) = \int_0^t dt' \int d\mathbf{x}' \mathcal{P}_2(\mathbf{x}', t')\mathcal{G}_{t-t'}(\mathbf{x}; \mathbf{x}')\mathcal{G}_{t-t'}(\mathbf{y}; \mathbf{x}'), \tag{5}$$

where $\mathcal{P}_2(\mathbf{x}, t) = \beta\nu_2\psi_t(\mathbf{x})$ is the average rate of appearance of particle pairs at position $\mathbf{x}$ and time t, the coefficient $\nu_2 = \sum_k k(k - 1)\, p_k$ being the mean number of pairs created at each fission [12]. For an exactly critical system, assuming again $q = 1/V$, we have $\mathcal{P}_2(\mathbf{x}, t) = \beta\nu_2\psi_0$, and the pair correlation function thus yields

$$h_t(\mathbf{x}, \mathbf{y}) = h_t^{id}(\mathbf{x}, \mathbf{y}) + \beta\nu_2\psi_0 \int_0^t dt' \mathcal{G}_{2t'}(\mathbf{x}; \mathbf{y}), \tag{6}$$

where we have used the Markov property of the Green's functions, namely,

$$\int d\mathbf{x}' \mathcal{G}_t(\mathbf{x}; \mathbf{x}')\mathcal{G}_t(\mathbf{y}; \mathbf{x}') = \mathcal{G}_{2t}(\mathbf{x}; \mathbf{y}). \tag{7}$$

Actually, it is customary to introduce the (dimensionless) normalized and centered pair correlation function g [11], namely,

$$g_t(\mathbf{x}, \mathbf{y}) = \frac{h_t(\mathbf{x}, \mathbf{y}) - h_t^{id}(\mathbf{x}, \mathbf{y})}{\psi_t(\mathbf{x})\psi_t(\mathbf{y})}. \tag{8}$$

When particles trajectories are very weakly correlated, $h_t(\mathbf{x}, \mathbf{y}) \sim h_t^{id}(\mathbf{x}, \mathbf{y})$ and thus $g_t \sim 0$: we will therefore have Poisson fluctuations. When $g_t \sim 1$, the typical local fluctuations will be comparable to the average local density ψ_t. From Eqs. (6) and (8), for an exactly critical system we have

$$g_t(\mathbf{x}, \mathbf{y}) = \frac{\beta\nu_2}{\psi_0} \int_0^t dt' \mathcal{G}_{2t'}(\mathbf{x}; \mathbf{y}). \tag{9}$$

The amplitude of g_t decreases with increasing particle density ψ_0 and with decreasing fission rate β, as expected on physical grounds.

IV. INCLUDING DELAYED NEUTRONS

The coupled stochastic evolution of neutrons and *precursors* can be modelled as a *multi-type* Galton-Watson reproduction process [2]: the parent neutron disappears and is replaced by a random number k_p of prompt neutrons, behaving as the parent particle, and a random number k_d of *precursors*, with joint probability p_{k_p,k_d} [1, 2]. We will denote by λ the rate at which a precursor decays to a delayed neutron. When delayed neutrons are considered, the system is critical if $\beta(\nu_p + \nu_d - 1) = \gamma$, where $\nu_p = \sum_{k_p,k_d} k_p p_{k_p,k_d}$ is the average number of prompt neutrons emitted per fission, and $\nu_d = \sum_{k_p,k_d} k_d p_{k_p,k_d}$ is the average number of precursors created per fission.

Similarly as done for prompt neutrons alone, we will assume that the neutron and precursor populations are at equilibrium within the box at $t = 0$. The analysis of the statistical moments of the neutron population in the presence of precursors can be again carried out by resorting to the backward approach based on probability generating functions. However, the multi-type branching process will give rise to a coupled system of two equations to be solved simultaneously (see the Appendix), and the resulting expressions for the moments are particularly cumbersome in their general form. Some simplifications can nonetheless be obtained by observing that the rate $\beta\nu_d$ at which precursors are created and the rate λ at which precursors are converted to delayed neutrons are actually strongly separated. Setting $\vartheta = \lambda/(\beta\nu_d)$, for typical nuclear systems we have $\vartheta \simeq 10^{-3}$ [1, 2]. This leads to the possibility of introducing singular perturbation techniques, which are amenable to physically meaningful results [15].

In particular, it is possible to show that for the average neutron density we have [14]

$$\psi_t(\mathbf{x}) \simeq \psi^p_{\vartheta t}(\mathbf{x}), \tag{10}$$

where $\psi^p_{\vartheta t}(\mathbf{x})$ is the average neutron density for a reactor that were to be run based on *prompt neutrons alone* (i.e., Eq. (3)). This means that in the presence of precursors the time evolution of ψ is slowed down by a factor ϑ. This behaviour is coherent with the classical findings in reactor control theory.

As for the normalized pair correlation function, for a critical system the precursors induce a stronger effect [14], namely,

$$g_t(\mathbf{x}, \mathbf{y}) \simeq \vartheta g^p_{\vartheta t}(\mathbf{x}, \mathbf{y}) \tag{11}$$

where g^p_t is the correlation function for a reactor that were to be run based on prompt neutrons alone (i.e., Eq. (9)). Precursors are therefore extremely effective in *quenching the spatial clustering* of the neutrons: the spatial correlation function of the neutron population has a much slower evolution in time ($t \to \vartheta t$), and its amplitude is further rescaled by a factor ϑ. A rigorous derivation can be found in [14]. Equations (10) and (11) allow transposing the results obtained for ψ^p and g^p_t to the case of systems run with both neutrons and precursors.

V. THE THERMODYNAMIC LIMIT

The so-called *thermodynamic limit* is attained by considering a large number $N \to \infty$ of particles in a large volume $V \to \infty$ [11, 12]. Suppose that the individuals are uniformly distributed in V at time $t = 0$, and impose that the limit average particle density $\psi_0 = N/V$ is finite. At criticality, the Green's function for a d-dimensional infinite system without delayed neutrons is the Gaussian density

$$\mathcal{G}_t(\mathbf{x}; \mathbf{x}_0) = \frac{e^{-\frac{r^2}{4Dt}}}{(4\pi Dt)^{d/2}}, \tag{12}$$

which spatially depends only on the relative particle distance $r = |\mathbf{x} - \mathbf{x}_0|$. The average particle density is stationary, namely, $\psi_t(\mathbf{x}) = \psi_0$ when starting from a flat initial condition $q = 1/V$. As for the pair correlation function, from Eq. (9) we get

$$g_t(r) = \frac{\beta\nu_2}{8\pi^{d/2} D\psi_0} r^{2-d} \Gamma_{d/2-1}\left(\frac{r^2}{8Dt}\right), \tag{13}$$

where $\Gamma_a(z) = \int_z^\infty e^{-u} u^{a-1} du$ is the incomplete Gamma function [11]. The asymptotic time behaviour of Eq. (13) depends on the dimension d: it is known that $g_t(r) \sim \sqrt{t}$ for $d = 1$, $g_t(r) \sim \log(t)$ for $d = 2$, and $g_t(r) \sim g_d(r)$ for $d > 2$,

$$g_d(r) = \frac{\beta\nu_2 \Gamma\left(\frac{d}{2} - 1\right)}{8\pi^{d/2} D\psi_0} r^{2-d} \tag{14}$$

being an asymptotic stationary spatial shape [11, 12]. This means that in low dimension $d \leq 2$ a critical multiplying system will eventually display clustering (g_t diverges), irrespective of the average particle density ψ_0. For $d \geq 3$, the amplitude of $g_d(r)$ can be reduced by acting on ψ_0, and clustering can be thus quenched. The dimension-dependent behaviour of $g_t(r)$ is basically a consequence of the Polya's theorem, which states that diffusion in unconstrained domains is very effective for $d > 2$ (for $d \leq 2$ particles have a finite probability of coming back to their starting point).

VI. CONFINED GEOMETRIES

We will now focus on particles evolving in a finite-size d-dimensional box of linear size L. For the sake of simplicity, we will neglect delayed neutrons. By evoking the separation of variables, $\mathcal{G}_t(\mathbf{x}; \mathbf{x}_0)$ can be expanded in terms of a discrete sum of eigenfunctions $\varphi_\mathbf{k}$ of the operator $\mathcal{L}^\dagger_{\mathbf{x}_0}$ [12], in the form

$$\mathcal{G}_t(\mathbf{x}; \mathbf{x}_0) = \sum_\mathbf{k} \varphi_\mathbf{k}(\mathbf{x}) \varphi^\dagger_\mathbf{k}(\mathbf{x}_0) e^{\alpha_\mathbf{k} t}, \tag{15}$$

where $\alpha_\mathbf{k}$ are the associated eigenvalues. The functions $\varphi^\dagger_\mathbf{k}(\mathbf{x}_0)$ can be explicitly derived from the completeness condition

$$\sum_\mathbf{k} \varphi_\mathbf{k}(\mathbf{x}) \varphi^\dagger_\mathbf{k}(\mathbf{x}_0) = \delta(\mathbf{x} - \mathbf{x}_0), \tag{16}$$

and imposing normalization. By applying Neumann boundary conditions, for the d-dimensional box we have

$$\varphi_\mathbf{k}(\mathbf{x}) = \prod_{i=1}^{d} \cos\left(\pi k_i \frac{x_i}{L}\right) \tag{17}$$

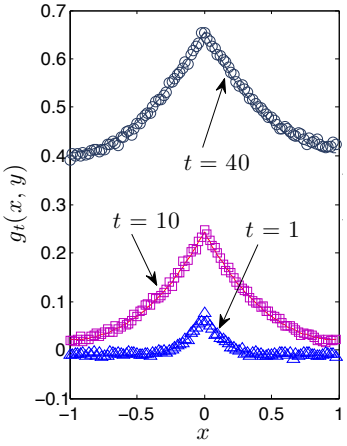

Fig. 2. The normalized and centered pair correlation function $g_t(x, y)$ for an initial collection of $N = 10^2$ branching Brownian motions with diffusion coefficient $D = 10^{-2}$ and birth rate $\beta = 1/2$ in a one-dimensional box of size $L = 2$. We take $y = 0$ and plot $g_t(x, y = 0)$ at times $t = 1$ (blue triangles), $t = 10$ (magenta squares) and $t = 40$ (grey circles). Symbols correspond to Monte Carlo simulations with 10^5 realizations, solid lines to exact solutions (Eq. (9)).

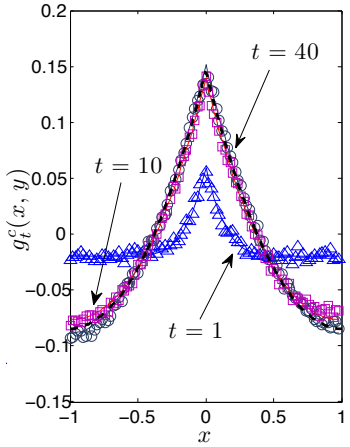

Fig. 3. The normalized and centered pair correlation function $g_t^c(x, y)$ for an initial collection of $N = 10^2$ branching Brownian motions with diffusion coefficient $D = 10^{-2}$ and birth rate $\beta = 1/2$ in a one-dimensional box of size $L = 2$. We take $y = 0$ and plot $g_t^c(x, y = 0)$ at times $t = 1$ (blue triangles), $t = 10$ (magenta squares) and $t = 40$ (grey circles). Symbols correspond to Monte Carlo simulations with 10^5 realizations, solid lines to exact solutions (Eq. (29)). At later times, $g_t^c(x, y = 0)$ converges to an asymptotic shape, displayed as a black dashed curve (Eq. (30)).

and

$$\alpha_{\mathbf{k}} = -D \sum_{i=1}^{d} \frac{\pi^2 k_i^2}{L^2} + \beta(\nu_1 - 1) - \gamma, \tag{18}$$

so that the fundamental eigenstate is spatially flat, and the associated fundamental eigenvalue is $\alpha_{\mathbf{0}} = \beta(\nu_1 - 1) - \gamma$.

For an exactly critical system, $\alpha_{\mathbf{0}} = 0$. From Eq. 5, by resorting to the eigenfunction expansion and singling out the fundamental mode we get

$$\tilde{h}_t(\mathbf{x}, \mathbf{y}) = \psi_0^2 \frac{\beta\nu_2}{N} t + \mathcal{H}_t(\mathbf{x}, \mathbf{y}), \tag{19}$$

where

$$\mathcal{H}_t(\mathbf{x}, \mathbf{y}) = \beta\nu_2\psi_0 \sum_{\mathbf{k}\neq\mathbf{0}} \frac{1 - e^{-2|\alpha_{\mathbf{k}}|t}}{2|\alpha_{\mathbf{k}}|} \varphi_{\mathbf{k}}(\mathbf{x})\varphi_{\mathbf{k}}^{\dagger}(\mathbf{y}) \tag{20}$$

is a bounded function for large t [12].

Analysis of Eq. (19) shows that the spatial fluctuations are ruled by two distinct time scales: a *mixing time* $\tau_D = -\alpha_{\mathbf{1}} \propto L^2/D$ and an *extinction time* $\tau_E = N/(\beta\nu_2)$ [12]. The quantity τ_D physically represents the time over which a particle has explored the finite viable volume V by diffusion. The emergence of the time scale τ_D is a distinct feature of confined geometries (in the thermodynamic limit, $\tau_D \to \infty$). Because of a finite τ_D, the shape of the correlation function only weakly depends on dimension d. The quantity τ_E represents the time over which the fluctuations due to births and deaths lead to the extinction of the whole population. When the concentration $\psi_0 = N/V$ of individuals in the population is large (and the system is spatially bounded), it is reasonable to assume that $\tau_E > \tau_D$.

The shape of the rescaled $g_t(\mathbf{x}, \mathbf{y})$ depends on the interplay of τ_D and τ_E [12], as illustrated in Fig. 2. Immediately after the initial time, $g_t(\mathbf{x}, \mathbf{y})$ displays a peak at short distances $\mathbf{x} \simeq \mathbf{y}$, which mirrors the effects of local fluctuations responsible for spatial clustering. The amplitude of the peak is proportional to the dimensionless ratio $\xi = \beta\nu_2 L^2/(ND) \propto \tau_D/\tau_E$, which precisely reflects the competition between migration and reproduction: the amplitude is smaller for larger D and smaller β (for fixed L and N), and vice-versa. The width of the peak, which is related to the correlation length of the system, is governed by diffusion, and is a growing function of D. For times shorter than the mixing time τ_D, the amplitude of the peak grows due to births and deaths dominating over diffusion, whereas its width increases due to diffusion. When $t \gg \tau_D$, the particles have explored the entire volume, and $\mathcal{H}_t(\mathbf{x}, \mathbf{y})$ freezes into a tent-like shape

$$\mathcal{H}_\infty(\mathbf{x}, \mathbf{y}) = \lim_{t\to\infty} \mathcal{H}_t(\mathbf{x}, \mathbf{y}) = \beta\nu_2\psi_0 \sum_{\mathbf{k}\neq\mathbf{0}} \frac{\varphi_{\mathbf{k}}(\mathbf{x})\varphi_{\mathbf{k}}^{\dagger}(\mathbf{y})}{2|\alpha_{\mathbf{k}}|}. \tag{21}$$

The total number of neutrons in the reactor also undergoes global fluctuations, N being finite. This progressively lifts upwards the contribution $\mathcal{H}_\infty(\mathbf{x}, \mathbf{y})$ by a spatially flat term (associated to the fundamental mode) that diverges linearly in time as $\sim t/\tau_E$. Finally, for times larger than the extinction time τ_E, $g_t(\mathbf{x}, \mathbf{y}) > 1$ everywhere. This physically means that, no matter how dense is the population is at $t = 0$, neutrons are eventually doomed to extinction within $t \simeq \tau_E$: in this respect, statistical equilibrium at the critical point is "*a mathematical fiction*", as argued in [3]. Including delayed neutrons would not qualitatively change these findings. However, the extinction time $\tau_E \simeq \tau_E^p/\vartheta^2$ would be much longer than $\tau_E^p = N/(\beta\nu_2)$ corresponding to prompt neutrons alone [14].

VII. FLUCTUATIONS CLOSE TO CRITICALITY

Let us assume that the system is initially at equilibrium with respect to the spatial distribution, with $q = 1/V$, but criticality is not ensured, i.e., $\gamma \neq \beta(\nu_1 - 1)$. From Eq. (3) we have thus

$$\psi_t(\mathbf{x}) = \psi_0 e^{\alpha_0 t}. \tag{22}$$

The sign of the fundamental eigenvalue $\alpha_0 = \beta(\nu_1 - 1) - \gamma$ determines the asymptotic behaviour of the average particle density: when $\alpha_0 > 0$ the system is super-critical and the population diverges in time; when $\alpha_0 < 0$ the system is sub-critical and the population shrinks to zero. As for the pair correlation function, from Eq. (8) assuming again $q = 1/V$ we obtain

$$g_t(\mathbf{x}, \mathbf{y}) = \frac{\beta\nu_2}{\psi_0} e^{-\alpha_0 t} \int_0^t dt' e^{-\alpha_0 t'} \mathcal{G}_{2t'}(\mathbf{x}; \mathbf{y}), \tag{23}$$

The ultimate fate of the pair correlation function at long times depends on the rate α_0 at which the average population is increasing or decreasing. When $\alpha_0 > 0$, the pair correlation function for long times asymptotically converges to the constant

$$g_t(\mathbf{x}, \mathbf{y}) \to \frac{\beta\nu_2}{N\alpha_0}, \tag{24}$$

which means that fluctuations will be equally distributed at any spatial scale. The average population is exponentially increasing at a rate α_0, thus contributing to the mixing of the individuals: for sufficiently large N one typically expects the amplitude of the pair correlation function to be $g \ll 1$, and fluctuations to be safely neglected. However, it may still happen that $g \gg 1$, when the number of initial particles is $N \ll \beta\nu_2/\alpha_0$, i.e., basically for small perturbations around criticality, with $\alpha_0 \simeq 0$. This can be understood as a competition between the growth time constant $1/\alpha_0$ of the average population and the extinction time $\tau_E = N/(\beta\nu_2)$: if α_0 is rather small, strong correlations may have enough time to develop, despite the smoothing effect induced by the appearance of an increasing number of new particles. When $\alpha_0 < 0$, the pair correlation function at long times grows unbounded exponentially fast, as $g_t(\mathbf{x}, \mathbf{y}) \sim \exp(-\alpha_0 t)$: the average population is rapidly decreasing, which enhances the relative importance of fluctuations due to correlations.

VIII. THE EFFECTS OF POPULATION CONTROL

Multiplying systems are typically subject to physical counter-reactions, such as the Doppler effect, which enforce population control mechanisms on the neutron population [2]. The simplest way to model such requirement for an exactly critical system is to impose that the total number N of neutrons is preserved, by correlating birth and death events [7]: at each fission, a neutron disappears and is replaced by a random number $k \geq 1$ of descendants, and $k - 1$ other neutrons are simultaneously removed from the collection in order to ensure the conservation of total population. The quantity $\tau_R = N/(\nu_2\beta)$ for a constrained system represents the time over which the system has undergone a full population renewal, and all the individuals descend from a single common ancestor.

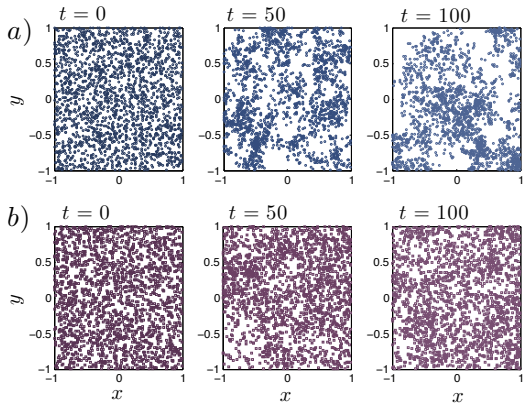

Fig. 4. Monte Carlo simulation of the evolution of branching Brownian motions in a two-dimensional box with reflecting boundaries, subject to population control. At $t = 0$, particles obey a uniform spatial distribution. In case *a*), the ratio ξ is close to unit and clustering phenomena dominate over diffusion (however, since the total particle number is preserved, the population can not go to extinction). In case *b*), the ratio ξ is ten times smaller and spatial fluctuations are much milder.

The pair correlation function $h_t^c(\mathbf{x}, \mathbf{y})$ in the presence of population control can be explicitly computed [13]. The probability for a chosen pair of particles at time t not to have had a common ancestor is $U(t) = e^{-\frac{\beta\nu_2}{N-1}t}$. The correlated contribution $\tilde{h}_t^c$ reads then

$$\tilde{h}_t^c(\mathbf{x}, \mathbf{y}) = \int_0^t dt' \int d\mathbf{x}' \mathcal{P}_2^c(\mathbf{x}', t', t) \mathcal{G}_{t-t'}(\mathbf{x}; \mathbf{x}') \mathcal{G}_{t-t'}(\mathbf{y}; \mathbf{x}') \tag{25}$$

where

$$\mathcal{P}_2^c(\mathbf{x}, t', t) = \beta\nu_2 \psi_{t'}(\mathbf{x}) U(t - t') \tag{26}$$

is the average rate of appearance of particle pairs at position $\mathbf{x}$ and time t' when the system is observed at time t, under the aforementioned constraint on the total population [13]. Imposing a uniform source $q = 1/V$ therefore yields

$$\tilde{h}_t^c(\mathbf{x}, \mathbf{y}) = \beta\nu_2\psi_0 \int_0^t dt' U(t') \mathcal{G}_{2t'}(\mathbf{x}; \mathbf{y}). \tag{27}$$

The correlation function can thus be written as

$$h_t^c = c_N \psi_t(\mathbf{x}) \psi_t(\mathbf{y}) U(t) + \psi_t(\mathbf{x}) \delta(\mathbf{x} - \mathbf{y}) + \tilde{h}_t^c, \tag{28}$$

and we finally get $h_t^c = h_t^{id} + \mathcal{H}_t^c(\mathbf{x}, \mathbf{y})$, where

$$\mathcal{H}_t^c(\mathbf{x}, \mathbf{y}) = \beta\nu_2\psi_0 \sum_{\mathbf{k} \neq \mathbf{0}} \frac{1 - e^{-\left(2|\alpha_\mathbf{k}| + \frac{\beta\nu_2}{N}\right)t}}{\frac{\beta\nu_2}{N} + 2|\alpha_\mathbf{k}|} \varphi_\mathbf{k}(\mathbf{x}) \varphi_\mathbf{k}^\dagger(\mathbf{y}) \tag{29}$$

is a bounded function for large t [13]. The diverging term in h_t has been thus suppressed by population control, which is coherent with the findings in [2] concerning the stabilizing effect induced by counter-reactions on neutron fluctuations.

The rescaled pair correlation function $g_t^c(\mathbf{x}, \mathbf{y})$ has two distinct regimes when population control is enforced, as illustrated in Fig. 3. Immediately after the initial time, $g_t^c(\mathbf{x}, \mathbf{y})$ displays a peak at short distances $\mathbf{x} \simeq \mathbf{y}$, which is the signature

of spatial clustering. The amplitude and the width of the peak have the same behaviour as for the function $g_t(\mathbf{x},\mathbf{y})$ detailed above. Nonetheless, since the number of particles is preserved, the positive correlations at the center of the box imply negative correlations close to the boundaries. The amplitude of the peak grows and its width increases for times shorter than the mixing time τ_D, analogously as in the previous case. However, global spatial fluctuations are intrinsically suppressed by N being fixed due to population control. For times larger than τ_D, $\mathcal{H}_t^c(\mathbf{x},\mathbf{y})$ converges to an asymptotic tent-like shape

$$\mathcal{H}_\infty^c(\mathbf{x},\mathbf{y}) = \lim_{t\to\infty} \mathcal{H}_t^c(\mathbf{x},\mathbf{y}) = \beta\nu_2\psi_0 \sum_{\mathbf{k}\neq\mathbf{0}} \frac{\varphi_{\mathbf{k}}(\mathbf{x})\varphi_{\mathbf{k}}^\dagger(\mathbf{y})}{\frac{\beta\nu_2}{N} + 2|\alpha_{\mathbf{k}}|}. \quad (30)$$

In this regime, the spatial fluctuations are bounded by

$$|h^c(\mathbf{x},\mathbf{y})| \leq h_t^{id}\left[1 + \frac{d}{3}\xi\right]. \quad (31)$$

In order for the fluctuations to be small and prevent the emergence of spatial clustering, we must therefore have $\tau_D \ll \tau_R$, which occurs when the typical spatial separation between particles is thoroughly explored within a single generation (see Fig. 4). In a critical system with population control, spatial clustering can be quenched by simply imposing that N is sufficiently large, for arbitrary values of the other physical parameters.

IX. SPATIAL CLUSTER DISTRIBUTIONS

The spatial shape of the particle clusters can be characterized in terms of several moments, namely, the square center of mass

$$\langle r_{com}^2\rangle(t) \equiv \left\langle \left| \frac{1}{N}\sum_i \mathbf{r}_i(t) \right|^2 \right\rangle, \quad (32)$$

the mean square displacement

$$\langle r^2\rangle(t) \equiv \frac{1}{N}\sum_i \langle|\mathbf{r}_i(t)|^2\rangle, \quad (33)$$

and the mean square distance between pairs of particles

$$\langle r_p^2\rangle(t) \equiv \frac{1}{N(N-1)}\sum_{i,j}\left\langle|\mathbf{r}_i(t)-\mathbf{r}_j(t)|^2\right\rangle, \quad (34)$$

where $\mathbf{r}_i(t)$ denotes the position of the i-th particle in the population. By construction, these three quantities are related to each other by an elegant formula [8]:

$$\langle r_{com}^2\rangle(t) + \frac{1}{2}\frac{N-1}{N}\langle r_p^2\rangle(t) = \langle r^2\rangle(t). \quad (35)$$

The spatial moments can be formally expressed in terms of the average particle density $\psi_t(\mathbf{x})$ and of the correlation function $h_t(\mathbf{x},\mathbf{y})$. In particular, for the mean square displacement we have

$$\langle r^2\rangle(t) = \frac{1}{N}\int |\mathbf{x}|^2\psi_t(\mathbf{x})d\mathbf{x}. \quad (36)$$

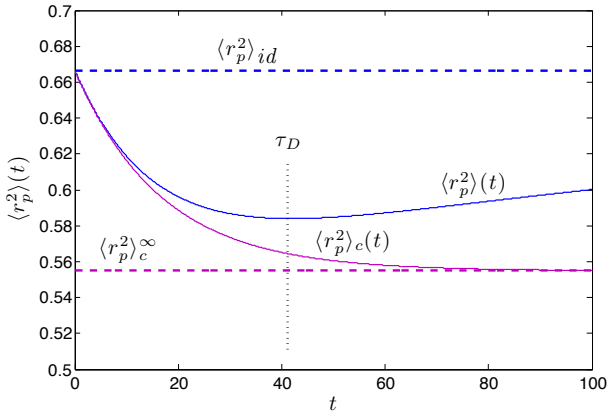

Fig. 5. The average square distance between particles $\langle r_p^2\rangle(t)$ for a one-dimensional model with $N = 10^2$ initial neutrons, $\beta = 1/2$, $D = 10^{-2}$, $\nu_2 = 1$ and $L = 2$. Blue solid curve: no population control. At long times, $\langle r_p^2\rangle(t)$ asymptotically converges to $\langle r_p^2\rangle_{id} = (1/6)L^2$ for a spatially uniform population, displayed as a blue dashed line. Magenta solid line: population control. At long times, $\langle r_p^2\rangle_c(t)$ asymptotically converges to $\langle r_p^2\rangle_c^\infty$ given in Eq. (40), displayed as a magenta dashed line.

For a critical system with $q = 1/V$, $\langle r^2\rangle(t)$ yields

$$\langle r^2\rangle(t) = \frac{1}{L^d}\int |\mathbf{x}|^2 d\mathbf{x} = \frac{d}{12}L^2. \quad (37)$$

As for the mean square distance between pairs of particles, we have

$$\langle r_p^2\rangle(t) = \frac{\int d\mathbf{x}\int d\mathbf{y}|\mathbf{x}-\mathbf{y}|^2 h_t(\mathbf{x},\mathbf{y})}{\int d\mathbf{x}\int d\mathbf{y} h_t(\mathbf{x},\mathbf{y})}. \quad (38)$$

An uncorrelated population uniformly distributed in the box would give

$$\langle r_p^2\rangle_{id} = \frac{1}{L^{2d}}\int d\mathbf{x}\int d\mathbf{y}|\mathbf{x}-\mathbf{y}|^2 = \frac{d}{6}L^2. \quad (39)$$

Deviations of $\langle r_p^2\rangle(t)$ from the ideal behaviour $\langle r_p^2\rangle_{id}$ allow quantifying the impact of spatial clustering [8, 13, 5]. The behaviour of the average square distance between particles for a critical reactor is illustrated in Fig. 5. At time $t = 0$, the population is uniformly distributed and $\langle r_p^2\rangle(0) = \langle r^2\rangle_{id}$. For a system without population control, $\langle r_p^2\rangle(t)$ at first decreases due to spatial clustering; then, for times longer than τ_D, global correlations dominate: $\langle r_p^2\rangle(t)$ increases and asymptotically saturates again to the ideal average square distance. This can by understood by observing that h_t becomes spatially flat for $t \gg \tau_E$ (see Eq. (19)). When on the contrary population control is enforced, $\langle r_p^2\rangle_c(t)$ at first decreases due to the competition between diffusion and birth-death; for times $t \gg \tau_D$, $\langle r_p^2\rangle(t)$ eventually converges to an asymptotic value that can be computed exactly based on Eqs. (29) and (38):

$$\langle r_p^2\rangle_c^\infty = 4d\frac{L^2}{\xi}\left[1 - \sqrt{\frac{8}{\xi}}\tanh\left(\sqrt{\frac{\xi}{8}}\right)\right]. \quad (40)$$

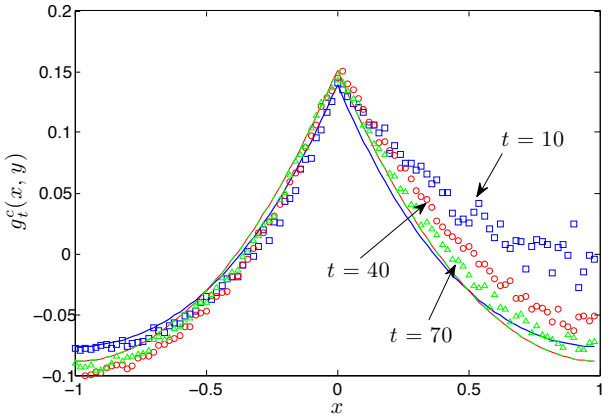

Fig. 6. The effects of perturbing the initial configuration q for a one-dimensional system with $N = 10^2$ neutrons, $\beta = 1/2$, $D = 10^{-2}$, and $L = 2$ ($\tau_D \simeq 40$). Population control is enforced. At $t = 0$, the neutrons are uniformly distributed in the left half-domain $[-1, 0]$. We display the time evolution of the pair correlation function $g_t^c(x, y = 0)$. Monte Carlo simulations with 10^5 realizations corresponding to the perturbed source are displayed as symbols: blue squares, $t = 10$; red circles, $t = 40$; green triangles, $t = 70$. Solid lines correspond to the analytical solutions of g_t^c starting from $q = 1/V$, taken at the same times. For $t \gg \tau_D$ the perturbation will be reabsorbed.

When spatial correlations are weak ($\xi \to 0$, which is obtained for a very large number of particles $N \to \infty$ or a vanishing fission rate $\beta \to 0$), from Eq. (40) we have

$$\langle r_p^2 \rangle_c^\infty \to \frac{d}{6} L^2 = \langle r_p^2 \rangle_{id} \tag{41}$$

and we recover the ideal case corresponding to uncorrelated trajectories. In this case, the center of mass of the population obeys

$$\langle r_{com}^2 \rangle_{id} = \langle r^2 \rangle - \frac{1}{2} \frac{N-1}{N} \langle r_p^2 \rangle_{id} = \frac{1}{N} \langle r^2 \rangle_{id}, \tag{42}$$

which basically means that for a collection of independent particles the mean square displacement of the center of mass is equal to the mean square displacement of a single particle of the collection, divided by the number of particles.

When the fission rate $\beta > 0$, we can expand Eq. (40) for a large but finite number of particles $N \gg 1$, which yields

$$\langle r_p^2 \rangle_c^\infty \simeq \langle r_p^2 \rangle_{id} \left[1 - \frac{\xi}{20} + \cdots \right]. \tag{43}$$

This result implies in particular that $\langle r_p^2 \rangle_\infty$ will be smaller than in the uncorrelated case because of the effects of spatial clustering. As for the center of mass, we finally get

$$\langle r_{com}^2 \rangle_c^\infty = \langle r_{com}^2 \rangle_{id} \left[1 + \frac{\xi}{20} + \cdots \right]. \tag{44}$$

Then, $\langle r_{com}^2 \rangle_c^\infty$ will be larger than that of an uncorrelated system.

X. PERTURBING THE INITIAL CONFIGURATION

So far, we have always assumed that the reactor was initially prepared on a spatial distribution proportional to the fundamental eigen-mode, i.e., $q = 1/V$, which was a convenient choice in view of more easily grasping the underlying physical mechanisms. Actually, Eq. (3) for the particle density and Eqs. (6) and (25) for the pair correlation function will hold true for arbitrary initial distributions $q(\mathbf{x}_0)$. Instead of considering the full evolution of ψ_t and h_t starting from a given source $q(\mathbf{x}_0)$, it is more instructive to address the relaxation to equilibrium starting from a given perturbed configuration, for an exactly critical system. Intuitively, the longest-lived perturbation will be obtained when the spatial distribution is proportional to the first excited eigen-mode $\varphi_{\mathbf{1}}$. Let us then assume that the perturbed source is written as

$$q^*(\mathbf{x}_0) = \frac{1}{V} \left[1 + \epsilon \varphi_{\mathbf{1}}(\mathbf{x}_0) \right], \tag{45}$$

where ϵ is the amplitude of the perturbation, taken so that $q^* \geq 0$. Normalization is trivially satisfied.

Let us now denote the perturbation of the average particle density by $\delta\psi_t(\mathbf{x}) = \psi_t^*(\mathbf{x}) - \psi_t^{eq}(\mathbf{x})$, where ψ_t^* corresponds to the perturbed source q^*, and ψ_t^{eq} corresponds to the equilibrium source $q = 1/V$. From Eq. (3), by resorting to the eigen-mode expansion in Eq. (15) and using orthogonality

$$\int d\mathbf{x} \varphi_{\mathbf{k}}(\mathbf{x}) \varphi_{\mathbf{k}'}^\dagger(\mathbf{x}) = \delta_{\mathbf{k},\mathbf{k}'}, \tag{46}$$

we get

$$\delta\psi_t(\mathbf{x}) = \epsilon \psi_0 \varphi_{\mathbf{1}}(\mathbf{x}) e^{\alpha_{\mathbf{1}} t} \tag{47}$$

where for a critical reactor $-\alpha_{\mathbf{1}} = 1/\tau_D$. This means that the perturbation $\delta\psi_t$ is reabsorbed exponentially fast, with a characteristic time scale equal to the mixing time τ_D: for times $t \gg \tau_D$, the average density asymptotically attains $\psi_t^* \to \psi_t^{eq}$.

As for the pair correlation function, let us similarly denote $\delta h_t = h_t^* - h_t^{eq}$. For a critical system without population control, from Eq. (3), by resorting to the eigen-mode expansion in Eq. (15) and using the orthogonality we get

$$\delta h_t(\mathbf{x}, \mathbf{y}) \simeq \psi_0 \left[\delta\psi_t(\mathbf{x}) + \delta\psi_t(\mathbf{y}) \right] \left(1 + \frac{t}{\tau_E} \right) \tag{48}$$

by neglecting terms converging faster. The perturbation δh_t is thus also reabsorbed exponentially fast, with a characteristic time scale τ_D. The linear correction is the signature of the diverging term induced by the critical catastrophe. For times $t \gg \tau_D$, the correlation function asymptotically attains $h_t^* \to h_t^{eq}$. When population control in enforced, from Eq. (25) we would get

$$\delta h_t^c(\mathbf{x}, \mathbf{y}) \simeq \psi_0 \left[\delta\psi_t(\mathbf{x}) + \delta\psi_t(\mathbf{y}) \right], \tag{49}$$

up to terms converging faster. The rate of convergence is the same as for the previous case, but the linear correction has disappeared. This behaviour is illustrated in Fig. 6 for a critical one-dimensional reactor.

XI. COARSE-GRAINING AND ENTROPY

So far, we have assessed the behaviour of the average particle density and of the pair correlation function by assuming that these quantities can be measured at any point $\mathbf{x}$ within the box. However, some coarse-graining procedure is introduced by the measurement techniques, which are typically performed over a finite-size detector volume [10, 11]. Suppose then that the d-dimensional box is partitioned into a regular Cartesian grid having M meshes, and denote by k_i the number of individuals found within a given mesh of index $i = 1, \cdots, M$. In the absence of branching ($\beta = 0$), the particle trajectories are independent: starting from a source $q = 1/V$ with N individuals, we would have

$$\langle k_i \rangle = \int_{V_i} d\mathbf{x} \psi_t(\mathbf{x}) = \frac{N}{M} \tag{50}$$

and

$$\sigma^2[k_i] = \int_{V_i} d\mathbf{x} \int_{V_i} d\mathbf{y} h_t^{id}(\mathbf{x}, \mathbf{y}) - \langle k_i \rangle^2 = \frac{N(M-1)}{M^2}, \tag{51}$$

for any index i, where we have used $V/V_i = M$. When $M \gg 1$, $\sigma^2[k_i] \simeq N/M$: independently diffusing particles lead to Poisson fluctuations, as expected. The *variance-to-mean ratio* $Y_i = \sigma^2[k_i]/\langle k_i \rangle = 1$ would not depend on the number of meshes used for coarse-graining [1, 2]. These results could have been equivalently obtained by remarking that at equilibrium the probability of finding k independently diffusing particles within any given mesh would be given by the Maxwell-Boltzmann distribution [2], namely,

$$P_{\mathcal{MB}}(k|N, M) = \binom{N}{k} \frac{(M-1)^{N-k}}{M^N}, \tag{52}$$

whence the average number of particles per cell

$$\langle k \rangle = \sum_k k P_{\mathcal{MB}}(k|N, M) = \frac{N}{M}, \tag{53}$$

and the variance

$$\sigma^2[k] = \sum_k k^2 P_{\mathcal{MB}}(k|N, M) - \langle k \rangle^2 = \frac{N(M-1)}{M^2}. \tag{54}$$

In the presence of clustering ($\beta > 0$), the result for the average number of particles would be left unchanged, whereas for the variance there would be position-dependent corrections due to spatial correlations [1, 2]. For the case of an exactly critical reactor without population control, we have

$$\sigma^2[k_i] = \frac{M-1}{M} \langle k_i \rangle + \langle k_i \rangle^2 \frac{\beta \nu_2}{N} t + \int_{V_i} d\mathbf{x} \int_{V_i} d\mathbf{y} \mathcal{H}_t(\mathbf{x}, \mathbf{y}),$$

whence an asymptotic variance-to-mean ratio

$$Y_i = \frac{M-1}{M} + \langle k_i \rangle \frac{\beta \nu_2}{N} t + \frac{\int_{V_i} d\mathbf{x} \int_{V_i} d\mathbf{y} \mathcal{H}_\infty(\mathbf{x}, \mathbf{y})}{\langle k_i \rangle} \tag{55}$$

[2] In the limit of large N and M, with finite $\mu = N/M$, $P_{\mathcal{MB}}$ can be approximated by a Poisson distribution with parameter μ.

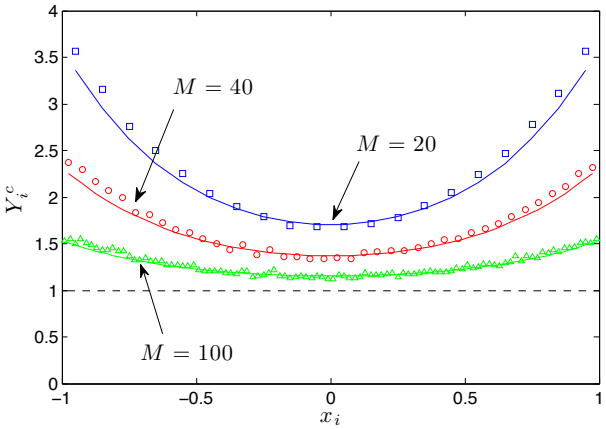

Fig. 7. The variance-to-mean ratio Y_i^c when population control is enforced: $N = 10^2$ particles evolve in a one-dimensional domain with size $L = 2$ and are observed at time $t = 70$, starting from $q = 1/V$. The physical parameters are $\beta = 1/2$ and $D = 0.01$, and $\tau_D \simeq 40$. Symbols represent Monte Carlo simulations with 10^5 realizations: blue squares for $M = 20$ meshes, red circles for $M = 40$ meshes, and green triangles for $M = 100$ meshes. Solid lines: exact formula (57). Dashed line: the limit case of pure diffusion, $Y_i = 1$.

for long times $t \gg \tau_D$. Since $\mathcal{H}_\infty(\mathbf{x}, \mathbf{y})$ is bounded, the variance-to-mean ratio will eventually diverge linearly in time and will be rather insensitive to the index i. When population control is enforced, we obtain

$$\sigma_c^2[k_i] = \frac{M-1}{M} \langle k_i \rangle + \int_{V_i} d\mathbf{x} \int_{V_i} d\mathbf{y} \mathcal{H}_t^c(\mathbf{x}, \mathbf{y}), \tag{56}$$

whence a bounded asymptotic variance-to-mean ratio

$$Y_i^c = \frac{M-1}{M} + \frac{\int_{V_i} d\mathbf{x} \int_{V_i} d\mathbf{y} \mathcal{H}_\infty^c(\mathbf{x}, \mathbf{y})}{\langle k_i \rangle} \tag{57}$$

with a non-trivial spatial structure, depending on the position of the mesh V_i within the box [10, 11]. Because of reflective boundary conditions, Y_i will be higher for meshes close to the boundaries, and lower for meshes close to the center of the box [12]. These findings are in agreement with the results discussed in [16] concerning the impact of reflective boundaries on correlations. Simple arguments show that $\int_{V_i} d\mathbf{x} \int_{V_i} d\mathbf{y} \mathcal{H}_\infty^c(\mathbf{x}, \mathbf{y}) \sim 1/M^2$, which implies that the corrections to Y_i^c due to correlations scale as

$$\frac{\int_{V_i} d\mathbf{x} \int_{V_i} d\mathbf{y} \mathcal{H}_\infty^c(\mathbf{x}, \mathbf{y})}{\langle k_i \rangle} \sim \frac{1}{M} \tag{58}$$

with respect to the number of meshes. A numerical example for a one-dimensional critical system is illustrated in Fig. 7.

In this context, a relevant question concerns the number of *empty cells* in the mesh. For a box with reflective boundaries partitioned into M meshes, in the absence of clustering it can be shown that the probability $R(s|N, M)$ of having exactly s empty cells for N diffusing particles asymptotically yields

$$R_{id}(s|N, M) = \binom{M}{s} \mathcal{S}_2(N, M-s) \frac{(M-s)!}{M^N}, \tag{59}$$

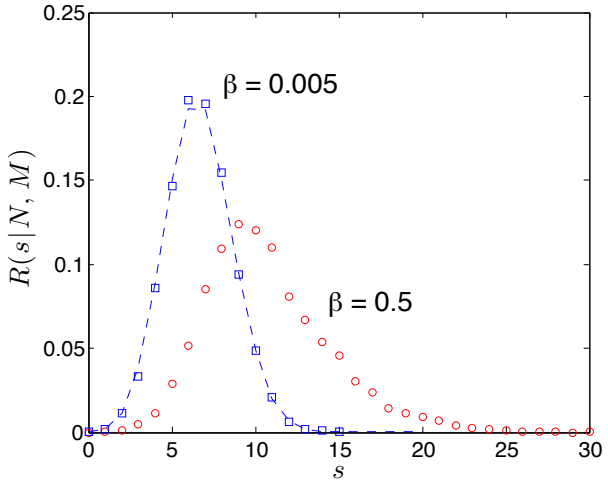

Fig. 8. The probability $R(s|N, M)$ of having s empty cells in the mesh, when population control is enforced: $N = 10^2$ particles evolve in a one-dimensional domain with size $L = 2$ and are observed at time $t = 70$, starting from $q = 1/V$. The physical parameters $D = 0.01$ and $\tau_D \simeq 40$. The number of meshes is $M = 50$. Symbols represent Monte Carlo simulations with 10^4 realizations: blue squares for $\beta = 5 \times 10^{-3}$ and red circles for $\beta = 1/2$. The dashed line is the distribution $R_{id}(s|N, M)$ corresponding to pure diffusion, as given by Eq. (59).

where $\mathcal{S}_2(n, i) = \frac{1}{i!}\sum_{j=0}^{i}(-1)^j\binom{i}{j}(i-j)^n$ are the Stirling numbers of the second kind. This result stems from the particles obeying a Maxwell-Boltzmann distribution for times $t \gg \tau_D$ when $\beta = 0$. In the limit of large N and M, with finite $\zeta = Me^{-N/M}$ (which basically means that the number of particles must be larger than the number of meshes, i.e., $N \gg M$), the exact distribution in Eq. (59) can be approximated by a Poisson distribution of parameter ζ. In the presence of fission-induced spatial correlations in a critical reactor, we expect s to increase with respect to the case of pure diffusion, because of clustering. Without population control, the number of empty cells will eventually saturate to $s \to M$ for times $t \gg \tau_E$, so that the asymptotic distribution will be trivial. When population control is enforced, the distribution $R(s|N, M)$ will convergence to some asymptotic shape at times $t \gg \tau_D$, with $\langle s\rangle$ larger than $\langle s\rangle_{id} \simeq \zeta$ obtained for diffusion. Monte Carlo simulations are displayed in Fig. 8 for a one-dimensional system.

A closely related physical observable is the ensemble-averaged Shannon *entropy*

$$\langle S\rangle = -\mathbb{E}\left[\sum_{i=1}^{M}\frac{k_i}{N}\log_2\left(\frac{k_i}{N}\right)\right], \tag{60}$$

where we have assumed that the probability of occupation of a cell of index i is estimated by k_i/N, since all the cells are equally accessible by diffusion. The entropy function $\langle S\rangle$ is supposed to provide a measure of the phase space exploration [5]. By construction, $0 \le \langle S\rangle \le \log_2(M)$, where the upper limit would correspond to an ideal repartition of particles uniformly within the box, in the limit of large N. For a purely diffusive system, from Eq. (52) we would obtain

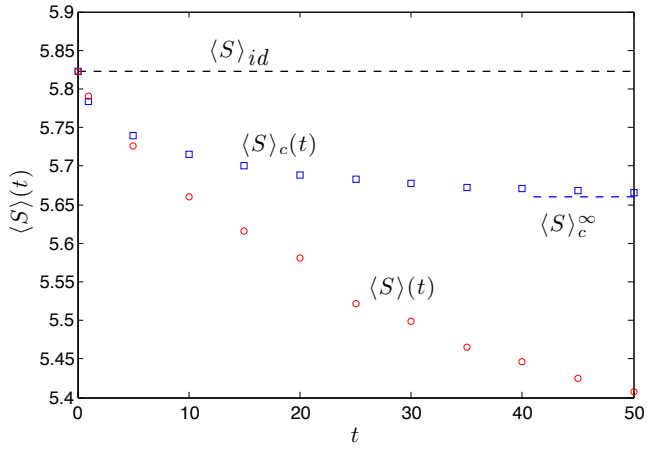

Fig. 9. The entropy $\langle S\rangle(t)$ as a function of time t, for $M = 100$ meshes: $N = 10^2$ particles evolve in a one-dimensional domain with size $L = 2$, starting from $q = 1/V$. The physical parameters $D = 0.01$ and $\tau_D \simeq 40$. Symbols represent Monte Carlo simulations with 10^4 realizations: blue squares with population control; red circles without population control. Black dashed line: the ideal case of pure diffusion, Eq. (61).

$$\langle S\rangle_{id} = \log_2(N) - \frac{M}{N}\sum_{k=0}^{N}P_{\mathcal{MB}}(k|N, M)k\log_2(k). \tag{61}$$

When N is large, $P_{\mathcal{MB}}(k|N, M)$ will be peaked around $\langle k\rangle = N/M$, and $\langle S\rangle_{id} \to \log_2(M)$. In the presence of spatial correlations, the entropy function will be lower than $\langle S\rangle_{id}$ because of clustering, as illustrated in Fig. 9. Monte Carlo simulations show that the behaviour of $\langle S\rangle_c$ when population control is enforced closely follows that of $\langle r_p^2\rangle_c$: for $t \gg \tau_D$, $\langle S\rangle_c$ will saturate to some asymptotic value $\langle S\rangle_c^\infty < \langle S\rangle_{id}$. Furthermore, we have a scaling $(\langle S\rangle_{id} - \langle S\rangle_c)/\langle S\rangle_{id} \sim M^{1/d}$ [5].

XII. CONCLUSIONS

We have illustrated the physical mechanisms that are responsible for neutron clustering in multiplying systems operated at and close to the critical point. The evolution of the spatial correlations dramatically depends on whether population control is enforced. To illustrate this point, exact formulas have been derived for a simple model of nuclear reactor and have been compared to Monte Carlo simulations.

XIII. ACKNOWLEDGMENTS

A. Zoia wishes to thank Électricité de France (EDF) for partial financial support.

APPENDIX: THE BACKWARD EQUATIONS

Consider a single walker starting from $\mathbf{x}_0$ at $t_0 = 0$. Let $n(\mathbf{x}, t|\mathbf{x}_0)$ be the number of particles found in $d\mathbf{x}$ close to $\mathbf{x}$ when the process is observed at $t > t_0$. It is convenient to introduce the associated two-volume probability generating

function

$$W_t(u, v|\mathbf{x}_0) = \mathbb{E}[u^{n(\mathbf{x},t|\mathbf{x}_0)} v^{n(\mathbf{y},t|\mathbf{x}_0)}]. \quad \text{(A.1)}$$

It can be shown that $W_t(u, v|\mathbf{x}_0)$ satisfies the backward equation

$$\frac{\partial}{\partial t} W_t = D\nabla^2_{\mathbf{x}_0} W_t - (\gamma + \beta) W_t + \gamma + \beta G[W_t], \quad \text{(A.2)}$$

where $G[z] = \sum_k p_k z^k$ is the probability generating function associated to p_k [12], in the absence of delayed neutrons.

Delayed neutron emission can be included by resorting to multi-type branching processes [1, 2]. The probability generating functions $W^n_t(u, v|\mathbf{x}_0)$ for a single neutron starting from $\mathbf{x}_0$ at $t_0 = 0$ and $W^c_t(u, v|\mathbf{x}_0)$ for a single precursor starting from $\mathbf{x}_0$ at $t_0 = 0$ satisfy the coupled system

$$\begin{aligned} \frac{\partial}{\partial t} W^n_t &= D\nabla^2_{\mathbf{x}_0} W^n_t - (\gamma + \beta) W^n_t + \gamma + \beta G^n[W^n_t] G^c[W^c_t] \\ \frac{\partial}{\partial t} W^c_t &= \lambda W^n_t - \lambda W^c_t, \end{aligned} \quad \text{(A.3)}$$

where $G^n[z]$ and $G^c[z]$ are the probability generating functions for the number of (prompt) neutrons and precursors at fission events, respectively.

Let us now consider a collection of N individuals initially located at $\mathbf{x}^1_0, \mathbf{x}^2_0, \mathbf{x}^3_0, \cdots, \mathbf{x}^N_0$ with density $Q(\mathbf{x}^1_0, \mathbf{x}^2_0, \cdots, \mathbf{x}^N_0)$ at time $t_0 = 0$. Assuming that particles evolve independently of each other, the probability generating function satisfies

$$W_t(u, v|\mathbf{x}^1_0, \mathbf{x}^2_0, \cdots, \mathbf{x}^N_0) = \prod_{k=1}^{N} W_t(u, v|\mathbf{x}^k_0). \quad \text{(A.4)}$$

Suppose that the initial positions are independently and identically distributed and obey the factorized density $Q(\mathbf{x}^1_0, \mathbf{x}^2_0, \cdots, \mathbf{x}^N_0) = \prod_{k=1}^{N} q(\mathbf{x}^k_0)$. The corresponding probability generating function $W_t(u, v|Q)$ satisfies then [12]

$$W_t(u, v|Q) = \left[\int_V d\mathbf{x}_0 q(\mathbf{x}_0) W_t(u, v|\mathbf{x}_0) \right]^N. \quad \text{(A.5)}$$

The m-th (factorial) moments of $n(\mathbf{x})$ and $n(\mathbf{y})$ can be obtained by derivation of $W_t(u, v|Q)$ with respect to u and v, respectively. In particular, the average particle number reads

$$\mathbb{E}[n(\mathbf{x}, t)] = \frac{\partial}{\partial u} W_t(u, v|Q)|_{u=1,v=1}. \quad \text{(A.6)}$$

For the two-volume correlations we take the mixed derivative, namely,

$$\mathbb{E}[n(\mathbf{x}, t) n(\mathbf{y}, t)] = \frac{\partial^2}{\partial u \partial v} W_t(u, v|Q)|_{u=1,v=1}. \quad \text{(A.7)}$$

In many practical applications, the initial number of particles is itself a random quantity K, with distribution $\mathcal{Z}(K)$. Assuming again independent and identically distributed coordinates $\mathbf{x}^k_0$, $k = 1, 2, \cdots, K$, Eq. (A.5) can be then generalized as

$$W_t(u, v|\mathcal{Z}) = \sum_K \mathcal{Z}(K) \prod_{k=1}^{K} \int_V d\mathbf{x}^k_0 q(\mathbf{x}^k_0) W_t(u, v|\mathbf{x}^k_0). \quad \text{(A.8)}$$

Often, the initial configuration is a Poisson point process [1]. In this case, the Campbell's theorem yields [1]

$$W_t(u, v|\mathcal{Z}) = \exp\left(N \int d\mathbf{x}_0 \left[W_t(u, v|\mathbf{x}_0) - 1 \right] q(\mathbf{x}_0) \right), \quad \text{(A.9)}$$

where we have set $N = \mathbb{E}[K]$ for the average number of source particles.

REFERENCES

1. I. PÁZSIT and L. PÁL, *Neutron Fluctuations: A Treatise on the Physics of Branching Processes*, Elsevier, Oxford (2008).
2. M. M. R. WILLIAMS, *Random processes in nuclear reactors*, Pergamon Press, Oxford (1974).
3. R. K. OSBORN and M. NATELSON, "Kinetic equations for neutron distributions," *Journal of Nuclear Energy Parts A/B*, **19**, 619–639 (1965).
4. I. PÁZSIT, "Duality in transport theory," *Annals of Nuclear Energy*, **14**, 25–41 (1987).
5. M. NOWAK, J. MIAO, E. DUMONTEIL, B. FORGET, A. ONILLON, K. SMITH, and A. ZOIA, "Monte Carlo power iteration: entropy and spatial correlations," *Annals of Nuclear Energy*, **94**, 856–868 (2016).
6. E. DUMONTEIL, F. MALVAGI, A. ZOIA, A. MAZZOLO, D. ARTUSIO, C. DIEUDONNÉ, and C. DE MULATIER, "Particle clustering in Monte Carlo criticality simulations," *Annals of Nuclear Energy*, **63**, 612–618 (2014).
7. Y.-C. ZHANG, M. SERVA, and M. POLIKARPOV, "Diffusion reproduction processes," *Journal of Statistical Physics*, **58**, 849–861 (1990).
8. M. MEYER, S. HAVLIN, and A. BUNDE, "Clustering of independently diffusing individuals by birth and death processes," *Physical Review E*, **54**, 5567 (1996).
9. W. R. YOUNG, A. J. ROBERTS, and G. STUHNE, "Reproductive pair correlations and the clustering of organisms," *Nature*, **412**, 328–331 (2001).
10. B. HOUCHMANDZADEH, "Neutral clustering in a simple experimental ecological community," *Physical Review Letters*, **101**, 078103 (2008).
11. B. HOUCHMANDZADEH, "Clustering of diffusing organisms," *Physical Review E*, **66**, 052902 (2002).
12. A. ZOIA, E. DUMONTEIL, A. MAZZOLO, C. DE MULATIER, and A. ROSSO, "Clustering of branching Brownian motions in confined geometries," *Physical Review E*, **90**, 042118 (2014).
13. C. DE MULATIER, E. DUMONTEIL, A. ROSSO, and A. ZOIA, "The critical catastrophe revisited," *Journal of Statistical Mechanics*, p. P08021 (2015).
14. B. HOUCHMANDZADEH, E. DUMONTEIL, A. MAZZOLO, and A. ZOIA, "Neutron fluctuations: the importance of being delayed," *Physical Review E*, **92**, 052114 (2015).
15. J. MIKA, "Two-particle correlations in reactor systems," *Annals of Nuclear Energy*, **2**, 59–66 (1975).
16. T. R. SUTTON, "Application of a Discretized Phase-Space Approach to the Analysis of Monte Carlo Uncertainties," *Nuclear Science and Engineering*, **185**, *1* (2017).